A newly formed shallow-contact binary RW Dor with new orbital period investigation

T. Sarotsakulchai[1,2,3], S.-B. Qian[1,2,4,5], B. Soonthornthum[3], E. Fernández Lajús[6,7], N.-P. Liu[1,4,5], X. Zhou[1,4,5], J. Zhang[1,4,5], W.-P. Liao[1,4,5], D. E. Reichart[8], J. B. Haislip[8], V. V. Kouprianov[8] and S. Poshyachinda[3]

huangbinghe@ynao.ac.cn

ABSTRACT

New CCD photometric light curves of short period (P=0.285d) eclipsing binary RW Dor are presented. The observations performed with the PROMPT-8 robotic telescope at CTIO in Chile from March 2015 to March 2017. The other eclipse timings were obtained from the 2.15-m JS telescope at CASLEO, San Juan, Argentina in December 2011. By light-curve analysis, it is found that RW Dor is a W-type shallow contact binary with a fill-out factor $f \sim 11\%$ and high mass ratio $q \sim 1.587$ ($1/\mathrm{q} = 0.63$), where the hotter component is the less massive one ($M_1 \sim 0.52M_\odot$ and $M_2 \sim 0.82M_\odot$). For orbital period investigation, the new fifteen eclipse times and those in previous published were compiled. Based on $O-C$ analysis with very weak evidence suggests that a long-term period decrease with a rate of $\mathrm{d}P/\mathrm{d}t = -9.61 \times 10^{-9}$ d yr^{-1} is superimposed on a cyclic variation ($A_3 = 0.0054$ days and $P_3 = 49.9$ yrs). The long-term period decrease can be interpreted as mass transfer from the more massive component to the less massive one or combine with the angular momentum loss (AML) via magnetic braking. In addition, with the marginal contact phase, high mass ratio ($1/\mathrm{q} > 0.4$) and the long-term period decrease, all suggest that RW Dor is a newly formed contact binary via a Case A mass transfer and it will evolve into a deeper normal contact binary. If the cyclic change is correct, the light-travel time effect via the presence of a cool third body will be more plausible to explain for this.

[1]Yunnan Observatories, Chinese Academy of Sciences, 650216 Kunming, China

[2]University of Chinese Academy of Sciences, 19 A Yuquan Rd., Shijingshan, 100049 Beijing, China

[3]National Astronomical Research Institute of Thailand, Ministry of Science and Technology, Bangkok, Thailand

[4]Key Laboratory of the Structure and Evolution of Celestial Objects, Chinese Academy of Sciences, 650216 Kunming, China

[5]Center for Astronomical Mega-Science, Chinese Academy of Sciences, 20A Datun Rd., Chaoyang District, Beijing, 100012, China

[6]Facultad de Ciencias Astronómicas y Geofísicas - UNLP, 1900 La Plata, Buenos Aires, Argentina

[7]Instituto de Astrofisica de La Plata - CONICET/UNLP, Argentina

[8]Department of Physics and Astronomy, University of North Carolina, CB #3255, Chapel Hill, NC 27599, USA

Subject headings: binaries: close - binaries: eclipsing - stars: evolution - stars: individual (RW Dor)

1. Introduction

RW Dor (HD 269320, HIP 24763) is an important binary for studying the formation and evolution at the beginning or newly formed contact binary after the common convective envelope has been formed and in transition either from detached or semi-detached to the contact phase. The system is a short-period W UMa-type binary with an orbital period of 0.285 days. A new period distribution for EW-type contact binaries was recently given by Qian et al. (2017). It was shown that the peak of the period distribution for this type of binary is near 0.29 days. This indicates that RW Dor is a typical W UMa-type contact binary. The system is near the Large Magellanic Cloud (LMC), but not a member of LMC as pointed out by Russo et al. (1984) and Marino et al. (2007). RW Dor was discovered as a variable star by Leavitt (1908) and later classified as a W UMa-type eclipsing binary by Hertzsprung (1925). The first spectral classification of the variable was made by Cannon (1921) who gave a spectral type of K5. This was subsequently confirmed by McLaughlin (1927) who also classified the system as a late-type eclipsing binary with the same spectral type.

The first photographic times of light minimum were reported by Hertzsprung (1928), who gave an orbital period of 0.143 days. Later, a lot of eclipse times were obtained by many authors (e.g. Russo et al. 1984; Marton et al. 1989; Kaluzny & Caillault 1989; Ogloza & Zakrzewski 2004; Marino et al. 2007) and the linear ephemeris of the binary was also corrected. The complete light curves were analysed with Wilson-Devinney method (Wilson & Devinney 1971) by Marton et al. (1989) and Kaluzny & Caillault (1989) who determined photometric elements independently. Those solutions indicated that RW Dor belongs to a W-subtype contact binary with components are not in poor thermal contact which predicted by the thermal relaxation oscillations theory (Lucy & Wilson 1979). Additionally, it was found that the light curves of RW Dor exhibited a significant difference in depths of the minima and showed variation. Marton et al. (1989) explained the asymmetry in the light curves as a hot spot on the cooler and more massive component located near the neck connecting the stars, while Kaluzny & Caillault (1989) reported that their light curves were only marginally asymmetric and did not show any scatter more than the observational errors.

The first radial-velocity measurements of RW Dor were published by Hilditch et al. (1992) with the 3.9-m telescope of Anglo-Australian Observatory. They found that RW Dor was composed of two K1 type stars and determined a spectroscopic mass ratio of $q_{sp} = 0.68$. By combining the photometric solutions given by Kaluzny & Caillault (1989), Hilditch et al. (1992) derived absolute parameters of the binary system. They confirmed that RW Dor is a W-subtype contact binary. The other radial-velocity curves were obtained by Duerbeck & Rucinski (2007) who determined a spectroscopic mass ratio of $q_{sp} = 0.63$. This is close to that derived by Hilditch et al. (1992). However, they found $V_0 = 25$ km/s that is quite smaller than the one ($V_0 = 66.5$ km/s) given by

Hilditch et al. (1992). Marino et al. (2007) reported that some light curves of RW Dor exhibited asymmetry, which were similar to the results published by Marton et al. (1989). They also re-computed the spectroscopic mass ratio by using the radial velocities given by Hilditch et al. (1992) and Duerbeck & Rucinski (2007). All eclipse times were also re-analyzed and they found a secular decrease in orbital period with a rate of $\Delta P/P \sim -6.3 \times 10^{-11}$. However, no light curve variation and third light in the system were found in recent publication (e.g. Deb & Singh 2011).

In this paper, we examine the variations of the light curve and determine new photometric solutions based on our CCD observations. Then, we compare our results to those from the other investigators. The orbital period changes are re-investigated with new eclipse times together with the others collected from the literature. Finally, the formation and the evolutionary state of the system, as well as the probability of the additional companion orbiting around the contact binary are all discussed.

2. CCD photometric observations

The first observations in V-band with two new times of light minimum were obtained by using the 2.15-m "Jorge Sahade" (JS) telescope at Complejo Astronomico El Leoncito (CASLEO), San Juan, Argentina during 9, 11 and 13 December 2011. During the observations, a VersArray 1300B camera was attached to the 2.15-m telescope with exposure 1095, 1300 and 1000 images for 2011 December 9, 11 and 13, respectively. The second observations in $BV(RI)_C$ bands were obtained from March 2015 to March 2017 by using the back illuminated Apogee F42 2048×2048 CCD photometric system, attached to the 0.60-m Cassegrain reflecting telescope of PROMPT-8[1] robotic telescope, which is located at the Cerro Tololo Inter-American Observatory (CTIO) in Chile. The web-based SKYNET client allowed us to request and retrieve image remotely via the internet. It also provided nightly calibration images, including bias, dark, and flat-field images (Layden & Broderick 2010). The CCD reduction and aperture photometry were done with standard

[1]PROMPT-8 is the Thai Southern Hemisphere Telescope (TST), operated in collaboration between National Astronomical Research Institute of Thailand (NARIT) and the University of North Carolina (UNC) at Chapel Hill in a part of the UNC-led PROMPT project, http://skynet.unc.edu.

Table 1: Coordinates of RW Dor, the comparison and the check stars.

Targets	Names	α_{2000}	δ_{2000}	V	R	J	H	K
Variable star	RW Dor	$05^{\rm h}18^{\rm m}32^{\rm s}.5$	$-68^\circ13'32''.7$	11.16	8.66	9.282	8.781	8.709
The comparison	GSC0916200441	$05^{\rm h}18^{\rm m}43^{\rm s}.6$	$-68^\circ07'33''.7$	12.25	11.89	11.916	11.859	11.863
The check	J05175264-6813241	$05^{\rm h}17^{\rm m}52^{\rm s}.6$	$-68^\circ13'24''.1$	12.33	11.27	10.782	10.285	10.169

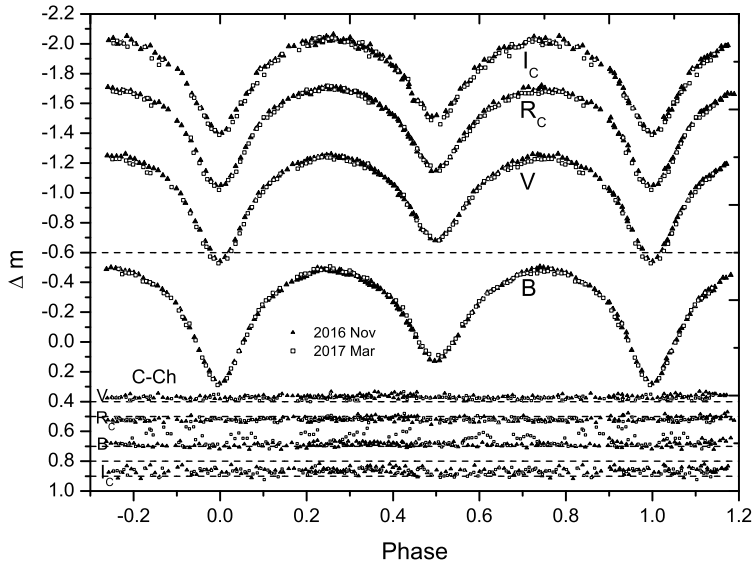

Fig. 1.— The two sets for second observation with complete light curves in B, V, R_c, I_c bands were obtained with the 0.6-m telescope at CTIO during November 2016 (dark triangles) and March 2017 (open squares). The differential magnitude between the comparison and check stars in BVR_cI_c bands (C-Ch) are plotted at the bottom of the figure and they were used to calibrate all data sets in each band.

procedure packages of IRAF[2]. The comparison star (C) is GSC 09162-00441; V= 12.25, $J-H$= 0.057 (SIMBAD) and the check star (Ch) is 2MASS J05175264-6813241; V= 12.33, $J-H$ = 0.497 (SIMBAD). The coordinates of those targets are listed in Table 1 and the complete multi-color light curves for second observation in November 2016 and in March 2017 are displayed in dark triangles and open squares of Fig. 1, respectively. The data from Fig.1 are listed in Table 2 for 2016 and Table 3 for 2017. The comparison of the two sets of light curves are also plotted together in the figure, they overlap nearly indicating that the light curves have no any changes and they are quite symmetric. The depths of the primary and the secondary minima of the two sets of light curves from Fig. 1 are displayed in Table 4 and no any significant changes were found there.

3. Orbital period investigations

The orbital period changes were analysed by using the $O-C$ method. All available eclipse times from the literature are collected and investigated together with new CCD photometric times from present observations listed in Table 5. The $O-C$ values of those eclipse times were computed by using the linear ephemeris given by Kreiner (2004);

$$Min.I(HJD) = 2451869.076 + 0^{\rm d}.2854633E. \tag{1}$$

To analyse the $O-C$ changes, we firstly use a quadratic ephemeris to fit the $O-C$ curve with weights 1 to photographic data (pg) and weights 10 to photoelectric (pe) or CCD data. The result is plotted as the solid line in the upper panel of Fig. 2. A least-squares solution leads to the following quadratic ephemeris:

$$\begin{aligned} &Min.I(HJD) = 2451869.07751(\pm0.00004) + 0.285462985(\pm0.000000002)E \\ &-[55.5(\pm0.2)\times10^{-13}]E^2. \end{aligned} \tag{2}$$

From the quadratic term in Eq. (2), the orbital period is decreasing and the change rate can be determined as ${\rm d}P/{\rm d}t = -14.19(\pm0.05)\times10^{-9}$ d yr^{-1}. The residuals from Eq. (2) are plotted in the lower panel of Fig. 2. As shown in in Fig. 2, we found that just only parabolic curve may not fit well, a cyclic variation seems to exist which can be seen clearly from the residuals in lower panel that are showing a large systematic scatter. Therefore, to get a better fit for the trend of $O-C$, a sinusoidal term is added to a quadratic ephemeris. By using a least-squares method, the ephemeris is re-determined as,

$$\begin{aligned} &Min.I(HJD) = 2451869.07786(\pm0.00004) + 0.285463214(\pm0.000000007)E \\ &-[37.6(\pm0.5)\times10^{-13}]E^2 \\ &+0.0054(\pm0.0001)\times\sin[0^\circ.00564E + 185^\circ.824(\pm0^\circ.684)]. \end{aligned} \tag{3}$$

As shown in Fig. 3, Eq. (3) can give a good description to the general trend of the $O-C$ curve. After the downward parabolic change is subtracted, the cyclic oscillation is displayed in

[2]The Image Reduction and Analysis Facility (IRAF), http://iraf.noao.edu.

Table 2: CCD observations of RW Dor in November 2016

HJD +2457700	ΔV	HJD	ΔR	HJD	ΔI	HJD	ΔV	HJD	ΔR	HJD	ΔI
20.5558	-1.228	20.5562	-1.641	20.5566	-2.017	20.8129	-1.061	20.8134	-1.522	20.8138	-1.894
20.5585	-1.233	20.5589	-1.664	20.5593	-1.991	20.8151	-1.090	20.8155	-1.531	20.8159	-1.906
20.5612	-1.238	20.5616	-1.681	20.5619	-2.039	20.8172	-1.099	20.8177	-1.539	20.8180	-1.918
20.5637	-1.250	20.5642	-1.676	20.5646	-2.037	20.8193	-1.116	20.8198	-1.557	20.8202	-1.928
20.5667	-1.255	20.5672	-1.692	20.5675	-2.039	20.8213	-1.117	20.8218	-1.567	20.8223	-1.921
20.5696	-1.260	20.5701	-1.686	20.5706	-2.023	20.8235	-1.147	20.8240	-1.580	20.8244	-1.949
20.5727	-1.238	20.5731	-1.675	20.5735	-2.029	20.8267	-1.158	20.8272	-1.604	20.8276	-1.965
20.5756	-1.234	20.5760	-1.688	20.5764	-2.012	20.8289	-1.183	20.8294	-1.633	20.8298	-1.987
20.5784	-1.232	20.5789	-1.659	20.5793	-2.015	20.8307	-1.194	20.8312	-1.648	20.8316	-1.990
20.5814	-1.225	20.5818	-1.656	20.5822	-2.042	21.5639	-1.271	21.5643	-1.709	21.5648	-2.039
20.5842	-1.210	20.5845	-1.656	20.5849	-2.003	21.5668	-1.265	21.5673	-1.704	21.5677	-2.054
20.5868	-1.220	20.5873	-1.656	20.5877	-1.966	21.5700	-1.265	21.5704	-1.687	21.5709	-2.015
20.5897	-1.190	20.5902	-1.630	20.5907	-1.978	21.5729	-1.264	21.5735	-1.688	21.5739	-2.024
20.5926	-1.175	20.5931	-1.613	20.5936	-1.973	21.5760	-1.282	21.5763	-1.677	21.5767	-2.067
20.5957	-1.170	20.5961	-1.608	20.5964	-1.957	21.5789	-1.256	21.5793	-1.687	21.5798	-2.042
20.5984	-1.137	20.5988	-1.601	20.5991	-1.921	21.5820	-1.249	21.5824	-1.663	21.5828	-2.012
20.6012	-1.123	20.6017	-1.573	20.6021	-1.901	21.5851	-1.220	21.5856	-1.661	21.5860	-1.979
20.6080	-1.077	20.6085	-1.507	20.6089	-1.861	21.5882	-1.220	21.5887	-1.629	21.5892	-1.994
20.6110	-1.049	20.6115	-1.491	20.6119	-1.821	21.5914	-1.194	21.5919	-1.628	21.5923	-2.003
20.6140	-0.984	20.6144	-1.463	20.6148	-1.815	21.5945	-1.184	21.5950	-1.605	21.5954	-1.954
20.6170	-0.975	20.6175	-1.401	20.6179	-1.783	21.5975	-1.172	21.5980	-1.609	21.5984	-1.921
20.6201	-0.927	20.6205	-1.373	20.6208	-1.709	21.6006	-1.138	21.6011	-1.579	21.6015	-1.913
20.6229	-0.855	20.6233	-1.311	20.6237	-1.618	21.6036	-1.114	21.6040	-1.560	21.6043	-1.876
20.6259	-0.845	20.6264	-1.256	20.6267	-1.613	21.6095	-1.050	21.6100	-1.483	21.6103	-1.846
20.6291	-0.757	20.6295	-1.223	20.6298	-1.597	21.6124	-1.016	21.6129	-1.453	21.6133	-1.818
20.6321	-0.735	20.6326	-1.184	20.6329	-1.526	21.6156	-0.952	21.6159	-1.394	21.6164	-1.746
20.6352	-0.694	20.6357	-1.126	20.6361	-1.512	21.6188	-0.897	21.6192	-1.351	21.6197	-1.680
20.6384	-0.682	20.6388	-1.130	20.6393	-1.520	21.6219	-0.828	21.6224	-1.285	21.6228	-1.615
20.6414	-0.686	20.6419	-1.160	20.6423	-1.480	21.6250	-0.772	21.6255	-1.220	21.6259	-1.584
20.6446	-0.727	20.6451	-1.177	20.6454	-1.548	21.6285	-0.696	21.6290	-1.145	21.6295	-1.522
20.6477	-0.752	20.6483	-1.217	20.6486	-1.597	21.6317	-0.645	21.6322	-1.085	21.6325	-1.470
20.6509	-0.809	20.6513	-1.268	20.6517	-1.624	21.6349	-0.583	21.6354	-1.055	21.6358	-1.427
20.6540	-0.852	20.6545	-1.330	20.6549	-1.698	21.6384	-0.561	21.6389	-1.052	21.6394	-1.417
20.6573	-0.902	20.6576	-1.379	20.6581	-1.733	21.6417	-0.590	21.6421	-1.059	21.6425	-1.441
20.6603	-0.935	20.6608	-1.419	20.6612	-1.751	21.6450	-0.636	21.6455	-1.116	21.6458	-1.524
20.6636	-1.010	20.6639	-1.450	20.6644	-1.838	21.6482	-0.706	21.6487	-1.179	21.6491	-1.573
20.6668	-1.040	20.6673	-1.489	20.6677	-1.850	21.6515	-0.780	21.6519	-1.235	21.6524	-1.613
20.6701	-1.068	20.6706	-1.530	20.6709	-1.892	21.6548	-0.857	21.6553	-1.306	21.6557	-1.680
20.6732	-1.096	20.6737	-1.552	20.6741	-1.883	21.6582	-0.917	21.6586	-1.373	21.6591	-1.710
20.6765	-1.123	20.6769	-1.589	20.6773	-1.915	21.6616	-0.970	21.6621	-1.430	21.6625	-1.819
20.6797	-1.134	20.6802	-1.574	20.6806	-1.968	21.6637	-1.017	21.6642	-1.459	21.6646	-1.849
20.6830	-1.168	20.6835	-1.616	20.6839	-1.978	21.6670	-1.058	21.6675	-1.501	21.6678	-1.862
20.6863	-1.188	20.6868	-1.625	20.6870	-1.973	21.6703	-1.080	21.6708	-1.547	21.6713	-1.892
20.6894	-1.212	20.6899	-1.632	20.6904	-1.978	21.6738	-1.116	21.6742	-1.572	21.6747	-1.911
20.6928	-1.205	20.6932	-1.646	20.6936	-1.982	21.6773	-1.135	21.6778	-1.583	21.6782	-1.938
20.6961	-1.227	20.6966	-1.685	20.6970	-2.002	21.6793	-1.159	21.6797	-1.610	21.6802	-1.936
20.6994	-1.242	20.6998	-1.690	20.7002	-2.026	21.6827	-1.177	21.6832	-1.631	21.6837	-1.998
20.7026	-1.260	20.7031	-1.669	20.7036	-2.048	21.6863	-1.213	21.6868	-1.649	21.6872	-2.000
20.7060	-1.259	20.7065	-1.676	20.7069	-2.031	21.6898	-1.221	21.6903	-1.664	21.6906	-1.957
20.7080	-1.251	20.7085	-1.700	20.7089	-2.006	21.6917	-1.214	21.6922	-1.663	21.6926	-2.030
20.7538	-1.013	20.7542	-1.485	20.7546	-1.814	21.6938	-1.228	21.6944	-1.675	21.6948	-2.030
20.7563	-0.987	20.7568	-1.419	20.7573	-1.777	21.6959	-1.247	21.6964	-1.668	21.6969	-2.002
20.7591	-0.960	20.7596	-1.378	20.7601	-1.749	21.6979	-1.242	21.6985	-1.683	21.6989	-2.047
20.7617	-0.906	20.7621	-1.355	20.7625	-1.703	21.7003	-1.254	21.7008	-1.691	21.7013	-2.032
20.7651	-0.828	20.7656	-1.299	20.7660	-1.615	21.7028	-1.260	21.7032	-1.685	21.7037	-2.031
20.7895	-0.656	20.7900	-1.141	20.7904	-1.495	21.7050	-1.261	21.7055	-1.705	21.7059	-2.024
20.7915	-0.676	20.7920	-1.153	20.7923	-1.530	21.7075	-1.263	21.7081	-1.713	21.7084	-2.065
20.7937	-0.724	20.7942	-1.199	20.7946	-1.558	21.7099	-1.265	21.7104	-1.694	21.7108	-2.035
20.7970	-0.808	20.7975	-1.254	20.7980	-1.643	21.7122	-1.265	21.7127	-1.709	21.7131	-2.078
20.8002	-0.869	20.8007	-1.330	20.8010	-1.710	21.7145	-1.268	21.7150	-1.709	21.7155	-2.047

Table 3: CCD observations of RW Dor in March 2017

HJD +2457800	ΔV	HJD	ΔR	HJD	ΔI	HJD	ΔV	HJD	ΔR	HJD	ΔI
26.5331	-0.871	26.5335	-1.338	26.5339	-1.683	26.6569	-1.095	26.6433	-1.626	26.6699	-1.719
26.5353	-0.837	26.5356	-1.290	26.5359	-1.663	26.6645	-1.007	26.6695	-1.410	26.6717	-1.703
26.5374	-0.806	26.5378	-1.261	26.5381	-1.633	26.6691	-0.919	26.6713	-1.310	27.5323	-1.642
26.5396	-0.789	26.5401	-1.227	26.5404	-1.575	26.6731	-0.826	27.5319	-1.251	27.5350	-1.593
26.5420	-0.766	26.5424	-1.223	26.5428	-1.553	27.5342	-0.725	27.5346	-1.179	27.5373	-1.540
26.5479	-0.737	26.5484	-1.190	26.5487	-1.525	27.5365	-0.703	27.5370	-1.142	27.5397	-1.506
26.5503	-0.761	26.5507	-1.221	26.5511	-1.572	27.5388	-0.638	27.5393	-1.124	27.5420	-1.497
26.5526	-0.781	26.5530	-1.240	26.5534	-1.586	27.5412	-0.625	27.5416	-1.098	27.5450	-1.464
26.5548	-0.811	26.5552	-1.282	26.5556	-1.617	27.5443	-0.593	27.5447	-1.070	27.5511	-1.499
26.5571	-0.843	26.5575	-1.320	26.5579	-1.671	27.5503	-0.624	27.5507	-1.136	27.5537	-1.551
26.5593	-0.859	26.5596	-1.347	26.5600	-1.709	27.5529	-0.675	27.5533	-1.164	27.5564	-1.589
26.5639	-0.951	26.5642	-1.402	26.5646	-1.778	27.5556	-0.724	27.5561	-1.192	27.5591	-1.681
26.5659	-0.983	26.5662	-1.428	26.5666	-1.791	27.5583	-0.794	27.5588	-1.259	27.5619	-1.691
26.5680	-1.020	26.5684	-1.456	26.5688	-1.823	27.5611	-0.855	27.5615	-1.322	27.5646	-1.753
26.5700	-1.023	26.5705	-1.490	26.5708	-1.840	27.5637	-0.929	27.5642	-1.381	27.5672	-1.795
26.5728	-1.068	26.5732	-1.518	26.5736	-1.879	27.5665	-0.969	27.5668	-1.436	27.5699	-1.811
26.5748	-1.091	26.5753	-1.553	26.5756	-1.903	27.5691	-1.014	27.5695	-1.481	27.5722	-1.907
26.5776	-1.134	26.5781	-1.558	26.5784	-1.906	27.5714	-1.046	27.5719	-1.507	27.5746	-1.867
26.5804	-1.148	26.5808	-1.600	26.5812	-1.965	27.5738	-1.071	27.5742	-1.557	27.5769	-1.924
26.5824	-1.150	26.5828	-1.609	26.5831	-1.950	27.5761	-1.105	27.5765	-1.556	27.5792	-1.946
26.5845	-1.160	26.5849	-1.617	26.5853	-1.997	27.5784	-1.132	27.5789	-1.576	27.5815	-1.961
26.5868	-1.182	26.5872	-1.627	26.5876	-2.002	27.5808	-1.152	27.5811	-1.591	27.5838	-1.965
26.5916	-1.219	26.5919	-1.659	26.5923	-2.014	27.5830	-1.159	27.5834	-1.617	27.5863	-2.007
26.5935	-1.211	26.5940	-1.661	26.5942	-1.983	27.5853	-1.194	27.5858	-1.636	27.5975	-2.034
26.5954	-1.224	26.5958	-1.687	26.5960	-2.063	27.5967	-1.228	27.5971	-1.693	27.6002	-2.076
26.5976	-1.250	26.5980	-1.694	26.5984	-2.041	27.5994	-1.250	27.5998	-1.720	27.6030	-2.061
26.5998	-1.227	26.6002	-1.686	26.6006	-2.043	27.6021	-1.264	27.6025	-1.743	27.6058	-2.084
26.6022	-1.250	26.6025	-1.710	26.6028	-2.049	27.6049	-1.270	27.6054	-1.725	27.6083	-2.110
26.6044	-1.258	26.6049	-1.708	26.6052	-2.076	27.6077	-1.292	27.6081	-1.736	27.6111	-2.120
26.6067	-1.266	26.6071	-1.708	26.6074	-2.093	27.6102	-1.302	27.6107	-1.733	27.6133	-2.095
26.6089	-1.266	26.6092	-1.709	26.6096	-2.079	27.6125	-1.304	27.6130	-1.752	27.6169	-2.108
26.6110	-1.282	26.6114	-1.725	26.6117	-2.094	27.6162	-1.302	27.6165	-1.768	27.6191	-2.115
26.6132	-1.283	26.6137	-1.705	26.6140	-2.086	27.6183	-1.302	27.6187	-1.765	27.6214	-2.110
26.6155	-1.279	26.6159	-1.714	26.6162	-2.057	27.6206	-1.290	27.6211	-1.742	27.6276	-2.085
26.6177	-1.282	26.6182	-1.721	26.6186	-2.069	27.6268	-1.307	27.6272	-1.752	27.6299	-2.090
26.6201	-1.284	26.6204	-1.718	26.6208	-2.085	27.6291	-1.280	27.6295	-1.731	27.6322	-2.069
26.6223	-1.283	26.6228	-1.711	26.6231	-2.074	27.6314	-1.277	27.6318	-1.722	27.6349	-2.052
26.6268	-1.272	26.6249	-1.730	26.6253	-2.066	27.6341	-1.256	27.6346	-1.735	27.6371	-2.082
26.6291	-1.253	26.6273	-1.719	26.6276	-2.046	27.6363	-1.264	27.6367	-1.703	27.6393	-2.085
26.6313	-1.246	26.6295	-1.718	26.6321	-2.066	27.6408	-1.232	27.6389	-1.698	27.6415	-2.032
26.6336	-1.261	26.6317	-1.704	26.6391	-2.044	27.6430	-1.261	27.6413	-1.682	27.6438	-1.990
26.6382	-1.229	26.6340	-1.686	26.6437	-1.967	27.6666	-1.052	27.6435	-1.656	27.6484	-2.022
26.6406	-1.192	26.6387	-1.667	26.6485	-1.925	27.6689	-0.987	27.6480	-1.720	27.6521	-1.977
26.6428	-1.188	26.6410	-1.677	26.6507	-1.957						

Table 4: The depths of eclipse (differential magnitude) in each band.

Filters	Nov 2016 (pri, sec)	Mar 2017 (pri, sec)
ΔB (± 0.004)	0.280 0.127	0.288 0.089
ΔV (± 0.002)	-0.541 -0.682	-0.536 -0.681
ΔR_C(± 0.002)	-1.052 -1.158	-1.033 -1.151
ΔI_C(± 0.003)	-1.402 -1.491	-1.389 -1.487

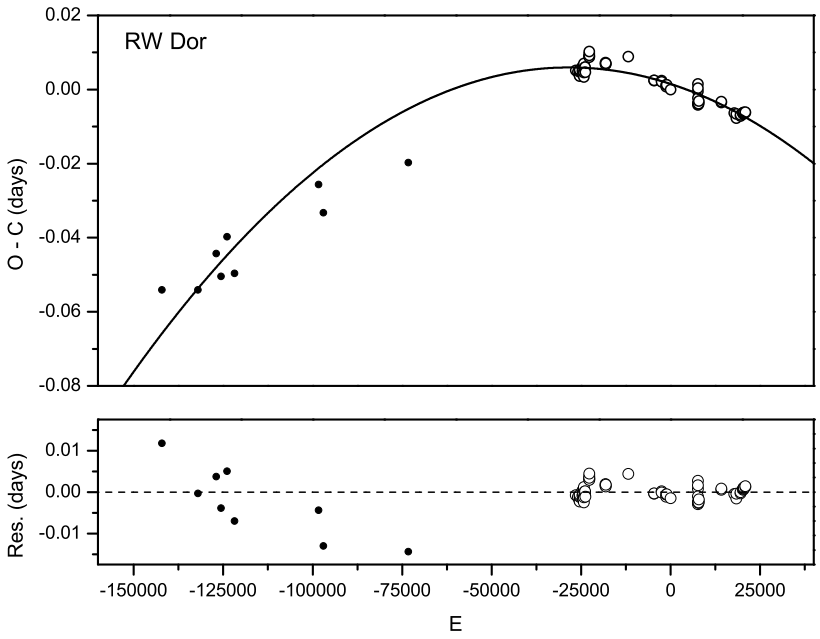

Fig. 2.— The $(O-C)$ curve. The dots before E = -50000 refer to photographic data (pg) and the open circles after E = -50000 refer to photoelectric (pe) and CCD data. The solid line in the upper panel was computed by using the quadratic term in Eq. (2) and this downward parabolic curve suggests a long-term period decrease. The residuals from Eq. (2) are plotted in the lower panel.

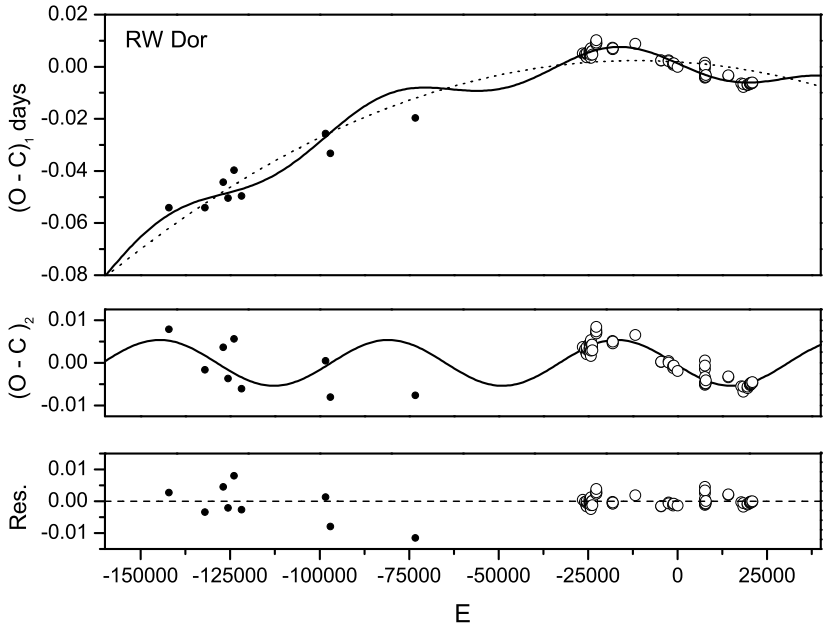

Fig. 3.— The $(O-C)_1$ diagram was constructed by using the ephemeris in Eq. (1). The solid line in upper panel refers to a combination of a long-term period decrease and a small-amplitude cyclic variation, while the dashed line represents the long-term decrease of the orbital period.

the middle panel. From this ephemeris, the sinusoidal term suggests that the semi-amplitude of cyclic variation is about 0.0054 days, while it has a long period of 49.92 years. The quadratic term also reveals a continuous period decrease at a rate of $\mathrm{d}P/\mathrm{d}t = -9.61(\pm0.13) \times 10^{-9}$ d yr^{-1} that is smaller than that derived from Eq. (2). The residuals from Eq. (3) are also plotted in the bottom panel of Fig. 3, its scatters are smaller than those in Fig. 2.

However, it cannot conclude that the result from Fig. 3 is better and reliable than Fig. 2. Because of small number of the $O-C$ data that are not cover (the gap between 1943 and 1980 or about 36.64 years) the whole cycles. Furthermore, the period of the third body from Fig. 3 is 49.92 years, while the total time span of available eclipse times only 127.48 years. Besides, the first nine minima (pre-1944) are photographic (pg) which listed in Table 3 with only three decimal places, thus they are ten times smaller weights when compared to the photoelectric (pe) and CCD data. Consequently, the effective time span of higher-quality minima (pe and CCD data) is only 37 years, less than the third body orbit period. Moreover, the point density (9 minima over a time interval of 53.81 years) for the first group is much lower than that of the second group (69 minima over a time interval of 37 years). For these reasons, the evidence for a sinusoidal term in Fig. 3 is very weak. The result from Eq. 2 may be possible for explanation of period change in RW Dor system. However, to check the period changes proposed here, more eclipse times are still required in the future to confirm the period variations.

4. Photometric solutions

As shown in Fig. 1, the two sets of light curves obtained in November 2016 and March 2017 overlap nearly. This suggests that the light curves are stable within the error during the time interval and no light curve variations are found. However, the light curves of some close binaries are asymmetric that could be explained by spot activity on one or both components (e.g., Qian et al. 2017a). For RW Dor, the light curves are quite symmetric indicating that they are useful to determine the photometric solutions of the binary. We model the two sets of light curves separately, i.e., set-1 refers to the one observed on 28-29 November 2016 and set-2 refers to the other obtained on 14-15 March 2017. The two data sets in B, V, R_c and I_c bands were analysed separately by using the Wilson & Devinney (W-D) code (Wilson & Devinney 1971; Wilson 1990, 1994, 2012; van Hamme & Wilson 2007).

Hilditch et al. (1992) classified the spectral type of the binary as K1 V following Marton et al. (1989). The Tycho-2 mean color index $B-V$=0.66 (Hog et al. 2000) corresponds to a spectral type of G4/5 V, while the color index in SIMBAD database reveals a $B-V=0.69$. For our solutions, the effective temperature of the primary star (T_1) was assumed at 5560 K according to its spectral type (Cox 2000). We assume that the convective envelopes are already developed. Thus, the bolometric albedos for star 1 and 2 were taken as $A_1 = A_2 = 0.5$ and the values of the gravity-darkening coefficients $g_1 = g_2 = 0.32$ were used. The monochromatic and bolometric limb-darkening coefficients were taken with logarithmic law from van Hamme's table (van Hamme

Table 5: Times of light minimum for RW Dor.

HJD (2400000+)	Error (days)	Method	Min. (type)	Ref.	HJD (2400000+)	Error (days)	Method	Min. (type)	Ref.
11298.835		pg	II	(1)	46681.7865	0.001	pe	II	(5)
14168.883		pg	II	(1)	46690.7785	0.0001	pe	I	(6)
15621.901		pg	II	(1)	46695.7745	0.0001	pe	II	(6)
16013.836		pg	II	(1)	48500.0470			I	(10)
16489.714		pg	II	(1)	50559.9437	0.0004	ccd	I	(7)
17075.903		pg	I	(1)	50560.0865	0.0003	ccd	II	(7)
23784.600		pg	I	(1)	51158.5603	0.0002	ccd	I	(7)
24172.537		pg	I	(1)	51158.7027	0.0002	ccd	II	(7)
30938.602		pg	I	(10)	51505.6820	0.0002	ccd	I	(7)
44313.581	0.001	pe	II	(2)	51505.8252	0.0002	ccd	II	(7)
44464.876	0.001	pe	II	(2)	51548.5020		ccd	I	(10)
44581.7728	0.0008	pe	I	(2)	51869.0760		ccd	I	(10)
44608.6063	0.0005	pe	I	(2)	54036.5947		ccd	I	(10)
44608.7488	0.0006	pe	II	(2)	54036.7411		ccd	II	(10)
44609.6063	0.0008	pe	II	(2)	54037.5995		ccd	II	(10)
44609.7493	0.0005	pe	I	(2)	54037.7384		ccd	I	(10)
44610.7487	0.0009	pe	II	(2)	54041.7335		ccd	I	(10)
44825.8462	0.0008	pe	I	(3)	54049.5878		ccd	II	(10)
44826.8442	0.0004	pe	II	(3)	54059.7177		ccd	I	(10)
44873.8038	0.0006	pe	I	(3)	54087.9783	0.0001	pe	I	(8)
44874.6594	0.0003	pe	I	(3)	54091.1189	0.0002	pe	I	(8)
44874.8010	0.0004	pe	II	(3)	54095.1150	0.0001	pe	I	(8)
44958.5851	0.0004	pe	I	(3)	54107.6761		ccd	I	(10)
44961.5843	0.0006	pe	II	(3)	55904.66718	0.00005	ccd	I	(9)
44961.7239	0.0006	pe	I	(3)	55906.80840	0.00005	ccd	II	(9)
44962.5815	0.0007	pe	I	(3)	56950.7446		ccd	II	(10)
44962.7267	0.0005	pe	II	(3)	57112.6009	0.0001	ccd	II	(9)
45021.6738	0.0003	pe	I	(3)	57118.5968	0.0001	ccd	II	(9)
45049.5058	0.0006	pe	II	(3)	57446.7363	0.0001	ccd	I	(9)
45049.6486	0.0008	pe	I	(3)	57447.5930	0.0001	ccd	I	(9)
45050.6484	0.0003	pe	II	(3)	57644.8485	0.0002	ccd	I	(9)
45076.4815	0.0004	pe	I	(3)	57645.8477	0.0001	ccd	II	(9)
45370.6556	0.0001	pe	II	(4)	57661.8334	0.0002	ccd	II	(9)
45370.6558	0.0003	pe	II	(4)	57686.6689	0.0003	ccd	II	(9)
45370.6564	0.0004	pe	II	(4)	57686.8119	0.0002	ccd	I	(9)
45376.6502	0.0001	pe	II	(4)	57720.6390	0.0002	ccd	II	(9)
45376.6507	0.0002	pe	II	(4)	57721.6383	0.0002	ccd	I	(9)
45376.6517	0.0002	pe	II	(4)	57826.5461	0.0002	ccd	II	(9)
46680.7878	0.001	pe	I	(5)	57827.5454	0.0002	ccd	I	(9)

Notes. (1) Hertzsprung 1928, (2) Marton & Grieco 1981, (3) Grieco & Marton 1983, (4) Russo et al. 1984, (5) Marton et al. 1989, (6) Kaluzny & Caillault 1989, (7) Ogloza & Zakrzewski 2004, (8) Marino et al. 2007,(9) the present authors, (10) http://var.astro.cz/ocgate.

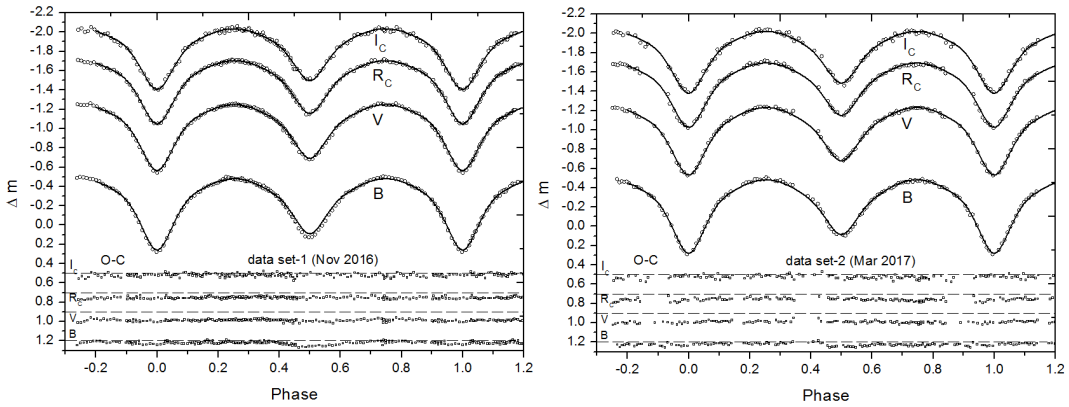

Fig. 4.— Theoretical light curves (solid lines) computed using the W-D method compared to the observed light-curves for data set-1 (left panel) and for data set-2 (right panel) without third light and spot. All synthetic light curves fit well with normal points except B-band light curves in data set-1 which is not fit well at the secondary minimum.

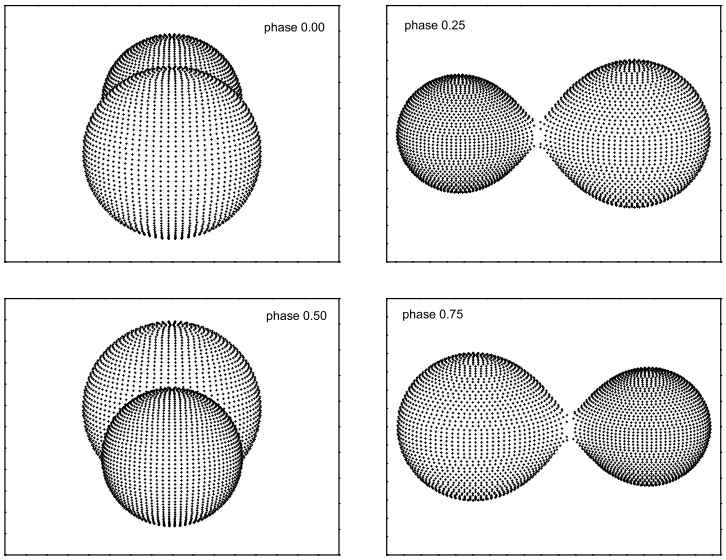

Fig. 5.— Geometrical structures at phases of 0.00, 0.25, 0.50 and 0.75

1993). All fixed parameters are listed in Tables 4. The adjustable parameters are the inclination (i), the mass ratio (q), the temperature of star 2 (T_2), the monochromatic luminosity of star 1 (L_{1B}, L_{1V}, L_{1R_c} and L_{1I_c}), the dimensionless potential of star 1 ($\Omega_1 = \Omega_2$) in mode 3 for contact configuration.

For precise mass ratio determination, Hilditch et al. (1992) had published results of radial-velocity measurements and gave a mass ratio of $q_{sp} = 0.68 \pm 0.03$. Later, Duerbeck & Rucinski (2007) obtained $q_{sp} = 0.63 \pm 0.03$. However, we used a q-search method first with our photometric data to determine the photometric mass ratio (q_{ph}) and then set mass ratio as an adjustable parameter to get a better fit for data set-1 and set-2. We obtained the initial mass ratio at q = 1.6 and then the differential correction was performed until the final solutions were derived at the lowest sum of the weighted square deviations $\Sigma(W(O-C))^2$, hereafter Σ. The result is about q = 1.62±0.02 or $1/q$ = 0.615 (which is close to the spectroscopic mass ratio of 0.63 that derived by Duerbeck & Rucinski, 2007) for both data sets. However, it is obvious that both sets of light curves show partial eclipses ($i < 85$ deg) that theirs photometric mass ratios obtained by q-search may not be accurate as discussed by Terrell & Wilson (2005). Therefore, we use the spectroscopic mass ratio 0.63 or 1/0.63 = 1.587 for our fixed mass ratio in the modeling process. The light-curve modeling results with optimum parameters are listed in Table 6. The corresponding theoretical light curves (solid lines) were compared to the observed light curves as shown in Fig. 4 for data set-1 (left panel) and for data set-2 (right panel). Additionally, Fig. 3 shows a cyclic variation that may be caused by light-travel time effect via the presence of a third body. Therefore, we added the third light (l_3) as an adjustable parameter in order to check the luminosity contribution of such a third companion, but the results show the negative values for both data sets. This may suggest that if the third body really exists, it will be a very cool stellar companion. On the other hand, it may have no any companion orbiting the eclipsing pair. The presence of the third body will be discussed again in the next section. The geometrical structures of RW Dor based on the modeling are displayed in Fig. 5.

5. Discussions and conclusions

The two sets of complete multi-color light curves in $BV(RI)_c$ bands were obtained by using the PROMPT-8 robotic telescope at CTIO in Chile from March 2015 to March 2017. The other data in 2011 were obtained by using the 2.15-m telescope at CASLEO, San Juan in Argentina. We compare our results to the light curves published by Deb & Singh (2011), no O'Connell effect (O'Connell 1951) and light curve variations were found. The photometric solutions indicate that RW Dor is a W-subtype, shallow contact binary with a degree of contact more than 10% and a high mass ratio ($q \sim 1.587$ or 0.63), which indicates that the hotter component is the less massive one. The absolute dimensions of RW Dor are derived by using our photometric elements together with spectroscopic one by Duerbeck & Rucinski (2007), the results are: $M_1 = 0.52M_\odot$, $M_2 = 0.82M_\odot$, a=$2.03R_\odot$, $R_1 = 0.703R_\odot$, $R_2 = 0.881R_\odot$, $L_1 = 0.423L_\odot$ and $L_2 = 0.534L_\odot$. These parameters

Table 6: Photometric solutions for data set-1 and set-2 when T_1=5560 K.

Parameters	set-1	set-2
$T_1(K)$	5560	5560
$g_1 = g_2$	0.32	fixed
$A_1 = A_2$	0.50	fixed
$q(M_2/M_1)$	1.587	fixed
T_2 (K)	5287(±10)	5238(±13)
$T_1 - T_2$ (K)	273	322
T_2/T_1	0.951	0.942
$i(^o)$	77.2(±0.1)	76.9(±0.2)
Ω_{in}	3.091	3.091
Ω_{out}	2.732	2.732
$\Omega_1 = \Omega_2$	4.64(±0.04)	4.62(±0.03)
$L_1/(L_1 + L_2)(B)$	0.475(±0.006)	0.491(±0.006)
$L_1/(L_1 + L_2)(V)$	0.455(±0.005)	0.467(±0.005)
$L_1/(L_1 + L_2)(R_c)$	0.444(±0.005)	0.455(±0.005)
$L_1/(L_1 + L_2)(I_c)$	0.437(±0.005)	0.446(±0.004)
$r_1(pole)$	0.3222(±0.0013)	0.3242(±0.0014)
$r_1(side)$	0.3378(±0.0014)	0.3402(±0.0015)
$r_1(back)$	0.3740(±0.0015)	0.3777(±0.0018)
$r_2(pole)$	0.4057(±0.0053)	0.4069(±0.0048)
$r_2(side)$	0.4309(±0.0069)	0.4326(±0.0063)
$r_2(back)$	0.4635(±0.0102)	0.4658(±0.0093)
f	11.5%(±6.7%)	15.0%(±6.1%)
$\Sigma W_i(O-C)_i^2$	0.01641	0.01866

Table 7: Parameters of the tertiary component for RW Dor.

Parameters	Value	Error	Units
P_3	49.9207	0.0003	yrs
A_3	0.0054	0.0002	days
$a'_{12} \sin i'$	0.929	0.026	AU
$f(m)$	0.00032	0.00003	$M_\odot$
e_3	0.0	assumed	-
M_3 ($i' = 90°$)	0.087	0.002	$M_\odot$
a_3 ($i' = 90°$)	14.33	0.58	AU

are close to those recently derived by Deb & Singh (2011).

The downward parabolic curve in the $O-C$ diagram shows the orbital period decrease at a rate of $\mathrm{d}P/\mathrm{d}t = -14.19 \times 10^{-9}$ d yr^{-1} without sinusoidal term and $\mathrm{d}P/\mathrm{d}t = -9.61 \times 10^{-9}$ d yr^{-1} with a cyclic oscillation. The type of variations, i.e., a long-term decrease combined with a cyclic change, is commonly found in W UMa-type stars, for examples, V417 Aql (Qian 2003), V1139 Cas (Li et al., 2015a), MR Com (Qian et al. 2013a), BX Peg (Li et al. 2015b), V524 Mon (He et al. 2012), and V1073 Cyg (Tian et al. 2018). Some W-type contact binaries whose properties are similar to RW Dor are listed in Table 8, most of them are shallow contact binaries with decreasing period. The long-term period decrease can be explained either by the mass transfer from the more massive component to the less massive one or by the angular momentum loss (AML) via magnetic braking, or by the combination of both processes. If the long-term period decrease is due to conservative mass transfer, the mass transfer rate can be determined with the following well-known equation,

$$\frac{\dot{P}}{P} = -3\dot{M}_2(\frac{1}{M_1} - \frac{1}{M_2}) \tag{4}$$

The mass transfer rate is $\mathrm{d}M/\mathrm{d}t = 23.55 \times 10^{-9}\ M_{\odot}\mathrm{yr}^{-1}$ for the case of Eq. 2 and $\mathrm{d}M/\mathrm{d}t = 15.95 \times 10^{-9}\ M_{\odot}\mathrm{yr}^{-1}$ for the case of Eq. 3. The timescale of mass transfer can be computed as $M_2/\dot{M} \sim 3.48 \times 10^7$yr (or 35 Myr) for Eq. 2 and $M_2/\dot{M} \sim 5.14 \times 10^7$yr (or 51 Myr) for Eq. 3. While the time scale of period decrease $P/\dot{P} \sim 2.01 \times 10^7$yr (or 20 Myr) for Eq. 2 and $P/\dot{P} \sim 2.97 \times 10^7$yr (or 30 Myr) for Eq. 3. The thermal timescale of the more massive component is 46.43×10^6yr (or 46 Myr). Those timescales reveal that RW Dor is presently undergoing a slow mass transfer at the beginning stages of contact evolution with high mass ratio, shallow contact configuration and long-term orbital period decrease. In this way, the contact degree of the system will become higher and the system will evolve into a deeper contact binary. Another plausible explanation for long-term period decrease is AML via magnetic stellar wind and it can be determined by the following equation given by Bradstreet & Guinan (1994),

$$\dot{P} \approx -1.1 \times 10^{-8} q^{-1}(1+q)^2(M_1+M_2)^{-5/3}k^2 \times (M_1R_1^4 + M_2R_2^4)P^{-7/3}, \tag{5}$$

where k^2 is the gyration constant ranging from 0.07 to 0.15 for solar type stars. By adopting a value of $k^2 = 0.1$ (Bradstreet & Guinan 1994), the rate of orbital period decrease due to AML can be computed as $\mathrm{d}P/\mathrm{d}t = -33.2 \times 10^{-9}$ d yr^{-1}, in this case the timescale of period decrease is $P/\dot{P} \sim 8.598 \times 10^6$yr (or 8.6 Myr) which is about two times shorter than the timescale from Eq. 2 and three times from Eq. 3. This means that the conservative mass transfer may not satisfy to explain the secular period decrease or the mass transfer may be dynamical (Qian & Zhu 2002). To explain this, Qian (2001a) proposed that the rate of AML is changed depending on the depth of overcontact. When the period decrease, the separation between the components becomes closer and the depth of contact increases, causing common convective envelope (CCE) to become deeper and increase mixing in the CCE which may result to AML to be lower rate (Vilhu 1981; Smith 1984). If AML value is larger than the critical value of Rahunen (1981) and causes orbital period to decrease, the evolution of RW Dor will be on the AML-controlled stage. Based on period studies

by Qian (2001a), the evolution of RW Dor may be the combination of the thermal relaxation oscillation (TRO) and the AML changes through the variable depth of overcontact, e.g. V417 Aql (Qian 2003). In addition, the study by Marton et al. (1989) has shown that there is a hot spot on the cooler component located near the neck of the system, suggesting a secondary-to-primary mass transfer which has a good agreement with the long-term period decrease. This indicates that RW Dor is in the transition phase to W UMa and is at the beginning of the contact phase similar to VW Boot (Qian & Zhu 2002). If the orbital period decrease is caused by losing angular momentum through magnetic braking, this is in agreement with the conclusion derived by Qian et al. (2017b, 2018) that some EW-type contact binaries were formed from short-period EA-type systems via case A mass transfer (Bradstreet & Guinan 1994; Vilhu 1982). Based on spectroscopic observations with LAMOST (Qian et al. 2017b, 2018) reveal that short period EW binaries (P $<$ 0.4 d) have low metallicities, suggesting that EW-type binaries are old stellar populations and may be older than their long period cousins. This means that they have a longer pre-contact phase (Qian et al. 2017b). Moreover, the evolution study of low-mass contact binaries (LMCB) by Stepien & Gazeas (2012) indicates that the systems with low total mass (M $<$ 1.4 $M_{\odot}$) and short orbital period (P $<$ 0.3 d) have a long pre-contact phase that lasts for 8-9 Gyrs, while the contact phase takes only about 0.8 Gyr with low mass transfer rate. The situation of RW Dor has good agreements with the conclusions proposed by Stepien & Gazeas (2012) and Qian et al. (2017b, 2018) that the shallow-contact binary with short period (P $\sim$ 0.285 d), low total mass (M $\sim$ 1.34 $M_{\odot}$) and long-term period decrease is a newly formed contact binary, which is similar to V524 Mon (He et al. 2012), MR Com (Qian et al. 2013a), BI Vul (Qian et al. 2013b) and CSTAR 038663 (Qian et al. 2014a), with the beginning state of the contact phase or recently evolved into contact configuration after it spent a long time in pre-contact phase. In addition, the absolute parameters of RW Dor are quite close to V336 TrA (Kriwattanawong et al 2018, see Fig. 4), suggesting that the more massive component (the secondary) of RW Dor will locate near the ZAMS (the zero age main sequence), while the location of the less massive one should be close to the TAMS (the terminal age main sequence). This means that the less massive one has evolved to reach the TAMS, whereas the more massive one has not evolved. It may be due to the mass transfer between the components.

In addition, a cyclic oscillation superimposed on a secular term is usually found in W UMa type binaries (see Qian 2001b, Qian 2002). Therefore, it is possible that there may exist a periodic variation superimposed on a secular period decrease in the $O-C$ curve of RW Dor, even weak evidence as explained in section 3. If assuming that the periodic change in $O-C$ curve exists, by analysis of Eq. 3, the sinusoidal term reveals a cyclic change with a semi-amplitude of 0.0054 days and a period of 49.92 years. The periodic variations in W UMa binary stars are usually explained by the two ideas, one is the Applegate mechanism (Applegate 1992) via magnetic activity cycles at one or both components. The second idea is the light-travel time effect (Liao & Qian 2010; Han et al. 2016) via the presence of a third body.

The Applegate mechanism suggests that the cyclic change is caused by magnetic activity-driven variations in the quadrupole moment of solar-type components. Because RW Dor consists of G4/5

Table 8: Parameters of marginal contact binaries (W-type systems).

Star	Sp.	Period (days)	$1/q$	f (%)	dP/dt ($\times 10^{-}8$ d/y)	Cyclic	l_3	M_1 ($M_\odot$)	M_2 ($M_\odot$)	M_3 ($M_\odot$)	activities	Ref.
KIC 9532219	G9	0.1981	0.833	-	-52.7	yes	76%	-	-	0.09	spot	(1)
CC Com	K4/5	0.2207	0.527	16.7	-20.0	yes	-	0.37	0.71	0.066	-	(2)
BI Vul	K3	0.2518	0.964	8.7	-9.5	yes	no	0.72	0.75	0.30	spot	(3)
V336 TrA	K1	0.2668	0.716	15.7	-	-	-	0.65	0.91	-	spot	(4)
CSTAR 038663	K3	0.2671	0.893	10.6	-	yes	$< 1\%$	0.72	0.81	0.63/2.02	spot/flares	(5)
BM UMa	K	0.2712	0.540	17.0	-7.49	yes	-	0.50	0.92	0.25	-	(6)
BX Peg	G5	0.2804	0.372	23.1	-9.84	yes	no	0.38	1.02	0.22	spot	(7)
GSC 2765-0348	G4	0.2835	0.313	34.0	-	-	-	-	-	-	2 spots	(8)
V524 Mon	G5	0.2836	0.476	7.7	-.015	yes	no	0.50	1.10	0.26	no	(9)
LO Com	K0	0.2864	0.404	3.2	-11.8	yes	no	0.32	0.79	-	no	(10)
GSC 3526-01995	K2	0.2922	0.351	18.2	-	yes	no	0.28	0.80	0.57	spot	(11)
IK Boo	G2	0.3031	0.873	2.2	-21.7	yes	-	0.86	0.99	0.21	spot	(12)
V2284 Cyg	G7	0.3069	0.345	39.2	-29.7	yes	no	0.30	0.86	0.036	no	(13)
TY Boo	G3	0.3171	0.466	12.0	-2.99	yes	-	0.53	1.14	0.49	-	(14)
V1007 Cas	K0	0.3320	0.297	8.1	-17.8	-	1.1%	0.34	1.14	-	spot	(15)
V781 Tau	G0	0.3449	0.453	21.6	-6.01	yes	no	0.71	1.57	0.16	spot	(16)
V396 Mon	F8	0.3963	0.392	18.9	-8.57	yes	no	0.36	0.92	0.31	-	(17)
PP Lac	G6	0.4012	0.435	23.9	-	yes	no	0.51	1.18	0.21	no	(18)
MR Com	F5	0.4127	0.256	10.0	-53.0	yes	$< 1\%$	0.36	1.40	0.18	no	(19)
RW Dor	G4/5	0.2854	0.630	>10	-1.42	unclear	no	0.52	0.82	unclear	no	(20)

Notes. (1) Lee et al 2016, (2) Yang et al. 2009, (3) Qian et al. 2013b, (4) Kriwattanawong et al. 2018, (5) Qian et al. 2014a, (6) Yang et al 2009, (7) Lee et al. 2004 & 2009, (8) Samec et al. 2012,(9) He et al. 2012, (10) Zhang et al. 2016, (11) Liao et al. 2012, (12) Kriwattanawong et al. 2017, (13) Wang et al. 2017, (14) Yang et al. 2007, (15) Li et al. 2018, (16) Li et al. 2016, (17) Liu et al. 2011, (18) Qian et al. 2005, (19) Qian et al. 2013a, (20) present study.

V spectral type stars, it should show strong magnetic activity. If this is in the case, the quadrupole moment of the binary star can be determined from the equations given by Rovithis-Livaniou et al. (2000) and Lanza & Rodono (2002),

$$\Delta P = \sqrt{[1 - \cos(2\pi P/P_3)]} \times A_3 \tag{6}$$

and

$$\frac{\Delta P}{P} = -9\frac{\Delta Q}{Ma^2}, \tag{7}$$

where A_3 is the amplitude of the sinusoidal term in Eq. (3), P_3 is the magnetic activity period, R is the radius of the active star and a is the separation. The result is $\Delta P/P \sim 1.317 \times 10^{-6}$ and the quadruple moment for primary star $\Delta Q_1 = 3.07 \times 10^{48}$ g cm^2 and for secondary star $\Delta Q_2 = 4.84 \times 10^{48}$ g cm^2. These values for both components are lower than the typical values for active contact binary which ranging from 10^{51} to 10^{52} g cm^2. Thus, the cyclic oscillation in Fig. 3 cannot be interpreted by the result of Applegate mechanism. Furthermore, no spot activity cycles or light curve variations were found during the observations. The light curves may be stable for years (see Fig. 1) comparing to the previous publications, which suggests that there is very weak magnetic activity cycle at that time. Therefore, this period modulation may not be caused by magnetic activity cycle that happens normally in single solar-type stars. There are many contact systems that periodic variations cannot be explained by the Applegate mechanism as discussed by Qian et al. (2013b), but the most probable reason causing the cyclic changes for those binaries is the light-travel time effect due to the perturbations from a third body (Irwin 1952, Borkovits & Hegedues 1996, Liao & Qian 2010).

Therefore, the plausible idea for the cyclic period change is the light-travel time effect via the presence of a third body. By assuming that the tertiary component is moving in a circular orbit, the value of $a'_{12}\sin i'$ is computed as 0.929 au by using the relation $a'_{12}\sin i' = A_3 \times c$, where A_3 is the semi-amplitude of the $O-C$ oscillation, c is the speed of light and i' is the orbital inclination of the third component. Thus the mass function, the masses and the orbital radii of the third component in different inclination values can be determined with the following equation:

$$f(m) = \frac{4\pi^2}{GP_3^2} \times (a'_{12}\sin i')^3 = \frac{(M_3 \sin i')^3}{(M_1 + M_2 + M_3)^2}, \tag{8}$$

the corresponding values are displayed in Table 7. The mass function of the third body can be derived as $f(m) = 0.00032(\pm 0.00003)M_\odot$. The mass of the third body $M_3 \sin i' = 0.087(\pm 0.002)M_\odot$ and the orbital radius $a_3 = 14.33$ au. If the minimum mass of the third body is 0.087 $M_\odot$, the third body will be a very low-mass star, red dwarf or M-type star that is extremely small luminosity and difficult to detect. Since no third light was reported in the photometric studies (Marino et al. 2007 and Deb & Singh 2011) and no spectral lines of a third body were found (Rucinski et al. 2007). To check the third body, we also searched for the third light during the photometric solution, but the results showed negative values that means the contribution of the third light is very small comparing to the total light of the system. Since its mass is very small and locates very

far ($\sim$ 14.33 au) from the central binary system, thus it may not play an important role for the origin and evolution of the central binary by removing angular momentum from the inner system via Kozai cycle (Kozai 1962). In this way, RW Dor will normally evolve into contact phase without acceleration.

Based on section 3, there is very weak evidence for cyclic change in $O-C$ analysis of Fig. 3 because of a few eclipse timings before 1948 with large scatter and a big gap of time interval between 1943 and 1980. However, almost contact binaries were found to be triple or multiple systems (Pribulla & Rucinski 2006; D'Angelo et al 2006; Rucinski 2007) and one can see at Table 6, most of them have no third light in their light curves but show periodic variations in long-term period changes. Recently, a possible substellar object orbiting around the solar-like contact binary V2284 Cyg was firstly reported by Wang et al. (2017). Also in K-type shallow contact binary CC Com with very low mass $M_3 = 0.066M_\odot$ by Yang et al. (2009) and KIC 9532219 with $M_3 = 0.089M_\odot$ by Lee at el. (2016) or TX Cnc with $M_3 = 0.097M_\odot$ by Liu et al. 2007. More recently, the eclipsing binary Kepler-503 has been found that there is a brown dwarf or low-mass star with $M_3 = 0.075M_\odot$ orbiting around a subgiant star (Canas et al. 2018). Therefore, the existence of third body in the system cannot be ruled out completely. To prove that the invisible additional companion exists or not, long-term monitoring in photometric with new eclipse timings and spectroscopic observations are required.

This work is supported by the National Natural Science Foundation of China (No. 11503077). We would like to thank Dr. Wiphu Rujopakarn and NARIT for time allocation to use PROMPT-8 for our observations. More CCD observations were obtained with the 2.15-m "Jorge Sahade" (JS) telescope at Complejo Astronomico El Leoncito (CASLEO), San Juan, Argentina. This research has made use of the SIMBAD online database, operated at CDS, Strasbourg, France, NASA's Astrophysics Data System (ADS).

REFERENCES

Applegate, J. H. 1992, ApJ, 385, 621

Bokovits, T. & Hegedues, T. 1996, Astro. Space Sci., 120, 63

Bradstreet, D. H. & Guinan, E. F. 1994, ASP conf. Ser. (Interacting Binary stars), 56, 228

Canas, C. I., Bender, C. F., Mahadevan, S., et al. 2018, ApJS, 861, L4

Cannon, A. J. 1921, Harvard Bull., 754

Cox, A. N. 2000, Allen's Astrophysical Quantities(4th ed.; New York: Springer)

D'Angelo, C., van Kerkwijk, M. H. & Rucinski, S. M. 2006, AJ, 132, 650

Dai, Z.-B., Qian, S.-B., , 2009, ApJ, 703, 109

Deb, S. & Singh, H. P. 2011, MNRAS, 412, 1787

Duerbeck, H. W., & Rucinski, S. M. 2007, AJ, 133, 169

Han, C., Udalski, A., Sumi, T. Gould, A., et al. 2017, ApJ, 843, 59

Han, Z.-T., Qian, S.-B., Voloshina, I., Metlov, V. G., Zhu, L.-Y., Li, L.-J. 2016, RAA, 16, 156

He, J.-J., Wang, J.-J. & Qian, S.-B. 2012, PASJ, 64, 85

Hertzsprung, E. 1925, BAN, 77, 218

Hertzsprung, E. 1928, BAN, 146, 154

Hilditch, R. W., Hill, G., Bell, S. A. 1992, MNRAS, 255, 285

Hog, E., Fabricius, C., Makarov, V. V. et al. 2000, A&A, 355, 27

Irwin, J. B., 1952, ApJ, 116, 211

Kaluzny, J. 1986a, Acta Astron., 36, 105

Kaluzny, J. 1986b, Acta Astron., 36, 113

Kaluzny, J. 1986c, Acta Astron., 36, 121

Kaluzny, J. & Caillault, J.-P. 1989, Acta Astron., 39, 27

Kozai, Y. 1962, AJ, 67, 579

Kreiner, J. M. 2004, Acta Astron., 54, 207

Kriwattanawong, W., Sanguansak, N. & Maungkorn, S., 2017, PASJ, 69, 62

Kriwattanawong, W., Sarotsakulchai, T., Maungkorn, S., Reichart, D. E., et al. 2018, NewA, 61, 1

Lanza, A. F., & Rodono, M. 2002, AN, 323, 424

Layden, A. C. & Broderick, A. J. 2010, PASP, 122, 1000

Leavitt, H. 1908, Harvard Annals, 60, 100

Lee, J. W., Kim, S.-L., Lee, C.-U., Youn, J.-H., 2009, PASP, 121, 1366

Lee, J. W., Hong, K. S., Koo, J.-R., Park, J.-H. 2016, ApJ, 820, 1

Li, K., Gao, D.-Y., Hu, S.-M., Gu, D.-F., Jiang, Y.-G., Chen, X. 2016, Ap&PP, 361, 63

Li, K., Hu, S.-M., Guo, D.-F., Jiang, Y.-G., Gao, D.-Y., Chen, X., 2015a, NewA, 34, 217

Li, K., Hu, S.-M., Guo, D.-F., Jiang, Y.-G., Gao, D.-Y., Chen, X., 2015b, NewA, 41, 17

Li, K., Qian, S.-B., Hu, S.-M., He, J.-J. 2014, AJ, 147, 98

Li, K., Xia, Q.-Q., Hu, S.-M., Guo, D.-F., Chen, X. 2018, PASP, 130, 074201

Liao, W.-P. & Qian, S.-B. 2010, MNRAS, 405, 1930

Liao, W.-P. & Qian, S.-B. & Liu, N.-P. 2012, AJ, 144, 178

Liu, L., Qian, S.-B., Boonrucksar, S., Zhu, L.-Y. et al., 2007, PASJ, 59, 607

Liu, L., Qian, S.-B., Liao, W.-P., He, J.-J., Zhu, L.-Y., et al. 2011, AJ, 141, 44

Lucy, L. B. & Wilson, R. E. 1979, ApJ, 231, 502

Marino, B. F., Walker, W. S. G., Bembrick, C., Budding, E. 2007, PASA, 24, 199

Marton, S. F. & Grieco, A. 1981, IBVS, No. 1960

Marton, S. F. & Grieco, A. 1983, IBVS, No. 2346

Marton, S. F., Grieco, A., Sistero, R. F. 1989, MNRAS, 240, 931

McLaughlin, D. B. 1927, AJ, 38, 45

Mullan, D. J. 1975, ApJ, 198, 563

O'Connell D. J. K. 1951, Riverview Pub., 2, 85

Ogloza, W. & Zakrzewski, B. 2004, IBVS, No. 5507

Paczynski, B., Szczygiel, D. M., Pilecki, B., Pojmanski, G. 2006, MNRAS, 368, 1311

Pribulla, T. & Rucinski, S. M. 2006, AJ, 131, 2986

Qian, S.-B. 2001a, MNRAS, 328, 635

Qian, S.-B. 2001b, MNRAS, 328, 914

Qian, S.-B. 2002, A&A, 384, 908

Qian, S.-B. 2003, A&A, 400, 649

Qian, S.-B. & Zhu, L.-Y. 2002, ApJ, 568, 1004

Qian, S.-B., Zhu, L.-Y. & Boonrucksar, S. 2005, NewA, 11, 52

Qian, S.-B., Liu, N.-P., Liao, W.-P., He, J.-J., Liu, L., Zhu, L.-Y., Wang, J.-J., & Zhao, E.-G. 2013a, AJ, 146, 38

Qian, S.-B., Liu, N.-P., Li, K., He, J.-J., Zhu, L.-Y., Zhao, E.-G., et al. 2013b, ApJS, 209, 13

Qian, S.-B., Wang, J.-J., Zhu, L.-Y., Boonrucksar, S., et al. 2014a, ApJS, 212, 4

Qian, S.-B., Zhou, X., Zola, S., Zhu, L.-Y., et al. 2014b, AJ, 148, 79

Qian, S.-B., Han, Z.-T., Zhang, B., Zejda, M., Michel, R., Zhu, L.-Y., Zhao, E.-G., Liao, W.-P., Tian, X.-M., Wang, Z.-H., 2017a, ApJ, 848, 131

Qian, S.-B., He, J.-J., Zhang, J., Zhu, L.-Y., Shi, X.-D., Zhao, E.-G., Zhou, X. 2017b, RAA, 17, 87

Qian, S.-B., Zhang, J., He, J.-J., Zhu, L.-Y., Zhao, E.-G., Shi, X.-D.,Zhou, X., Han, Z.-T. 2018, ApJS, 235, 5

Qian, S.-B., Zhu, L.-Y., Zola, S., Liao, W.-P., et al. 2009a, ApJ, 695, L163

Qian, S.-B., Dai, Z.-B., Liao, W.-P., Zhu, L.-Y., et al. 2009b, ApJ, 706, L96

Qian, S.-B., Han, Z.-T., Soonthornthum, S., Zhu, L.-Y., et al. 2016, ApJ, 817, 151

Rahunen, T. 1981, A&A, 102, 81

Rovithis-Livaniou, H., Kranidiotis, A. N., Rovithis, P., Athanassiades, G. 2000, A&A, 354, 904

Rucinski, S. M. & Lu, W. 1999, AJ, 118, 2451

Rucinski, S. M., Pribulla, T. & van Kerkwijk, M. H. 2007, 134, 2353

Russo, G., Vittone, A. A., Milano, L. 1984, A&AS, 57, 69

Schmidtke, P. C., Cowley, A. P., Frattare, L. M., Mcgrath, T. K., et al. 1994, PASP, 106, 843

Smith, R. C. 1984, Q. JI R. Astro. Soc., 25, 405

Terrell, D. & Wilson, R. E. 2005, Ap&SS, 296, 221

Tian, X.-M., Zhu, L.-Y., Qian, S.-B., Li, L.-J., Jiang, L.-Q. 2018, RAA, 18, 20

Van Hamme, W. 1993, AJ, 106, 2096

Van Hamme, W. & Wilson, R. E. 2007, ApJ, 661, 1129

Vilhu, O. 1981, Ap&SS, 78, 401

Vilhu, O. 1982, A&A, 109, 17

Wang, J.-J., Qian, S.-B., He, J.-J., Li, L.-J., Zhao, E.-G. 2014, AJ, 148, 95

Wang, J.-J., Jiang, L.-Q., Zhang, B., Zhao, S.-Q., Yu, J. 2017, PASP, 129, 982, pp. 124202

Wilson, R. E. 1990, ApJ, 356, 613

Wilson, R. E. 1994, PASP, 106, 921

Wilson, R. E. 2012, AJ, 144, 73

Wilson, R. E. & Devinney, E. J. 1971, ApJ, 166, 605

Yang, Y.-G., Dai, J.-M. & Yin, X.-G. 2007, AJ, 134, 179

Yang, Y.-G., Lu, G.-L., Yin, X.-G., Zhu, C.-H., Nakajima, K. 2009, AJ, 137, 236

Yang, Y.-G., Wei, J.-Y., Nakajima, K. 2009, PASJ, 61, 13

Zhang, Y., Han, Q.-W. & Liu, J.-Z. 2016, PASP, 128, 124201